

A Simple Route to Morphology-Controlled Polydimethylsiloxane Films Based on Particle-Embedded Elastomeric Masters for Enhanced Superhydrophobicity

Dong-Wook Jeong,^{†,||} Seung-Jun Kim,^{†,||} Jong-Kweon Park,[§] Soo-Hyung Kim,^{†,‡} Deug-Woo Lee,^{†,‡} and Jong-Man Kim^{*,†,‡}

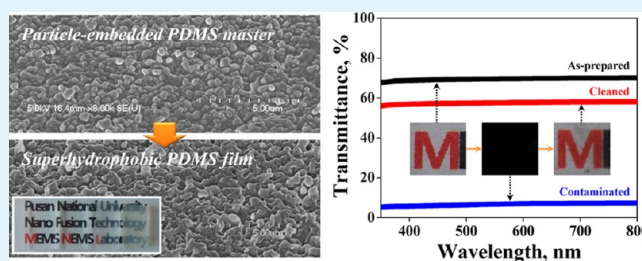
[†]Department of Nanofusion Technology and [‡]Department of Nanomechanics Engineering, Pusan National University, Busan 609-735, Republic of Korea

[§]Korea Institute of Machinery and Materials, Daejeon 305-343, Republic of Korea

Supporting Information

ABSTRACT: We present a simple route for controlling the surface morphology of polydimethylsiloxane (PDMS) films based on a standard replica molding technique incorporating a microparticle-embedded elastomeric master for enhancing surface wetting properties. The elastomeric masters are simply prepared by embedding microparticles (MPs) firmly into a surface of PDMS substrates using an abrasive air-jetting (AAJ) that can be potentially scaled up to large-area fabrication. The surface geometries of the PDMS masters can be easily controlled by using MPs with different shape and size in the AAJ process, resulting in easy control of the surface morphologies and resultant wetting and optical properties of the PDMS films after replicating. The PDMS masters are found to be highly durable, enabling repeated use to produce superhydrophobic PDMS films with similar characteristics. In addition, the fabricated PDMS films retain almost constant properties even under repetitive compressing and stretching deformations thanks to the mechanical robustness enabled by their all-elastomeric architectures. We show that the fabricated PDMS surfaces can be potentially employed as self-cleaning films in glass-based applications, even with complex surfaces, owing to their enhanced wetting properties, fairly good optical transparency, and superior mechanical stability.

KEYWORDS: particle-embedded PDMS masters, superhydrophobic PDMS films, abrasive air-jetting, mechanical robustness, self-cleaning capability



1. INTRODUCTION

Nature-inspired superhydrophobic surfaces have drawn considerable attention over the past years for industrial applications, demanding water-repellent surfaces, owing to their desirable surface effects such as self-cleaning, drag reduction, anti-icing, anti-bacterial adhesion, and so forth.^{1–12} In particular, the superhydrophobicity of such solid surfaces is mostly influenced by their surface roughness. Therefore, many efforts have been continually devoted to demonstrating functional surface structures by mimicking natural ones with unique surface physics through various fabrication techniques.^{2–6,13–17} More recently, research on artificial superhydrophobic surfaces has rapidly been moving toward the development of simple, scalable, and cost-effective fabrication methods, targeting to their practical applications. Moreover, the needs for mechanical durability and new functionalities such as mechanically flexible and optically transparent performance of the surfaces have been emphasized to expand potential applications, especially to curved or glass-based substrates. Proper material selection and the development of appropriate fabrication methods are very important factors. In this regard, polydimethylsiloxane (PDMS) is one of the most suitable structural materials for the

fabrication of functional surfaces mainly due to its mechanical/chemical stability, mechanical flexibility, optical transparency, and low surface energy. For this reason, a wide variety of approaches have been successfully developed to prepare PDMS-based superhydrophobic surfaces, which can be usually classified as either direct or indirect techniques depending on the fabrication methodologies.^{18–26} In direct techniques, the PDMS surfaces are physically modified to create the surface roughness mainly by direct nonlithographic methods including plasma etching,^{18–21} laser ablation,^{22–24} chemical corrosion,²⁵ layer formation,²⁶ and so forth. Although these techniques can be effective pathways to roughen the PDMS surfaces to enhance the wetting properties in a relatively simple manner, strict process conditions or apparatuses are inevitably required and must be controlled precisely to ensure process repeatability. In indirect approaches, a replica molding technique based on a well-established soft-lithographic process has been most widely used to produce surface structures on PDMS

Received: November 22, 2013

Accepted: January 23, 2014

Published: January 23, 2014

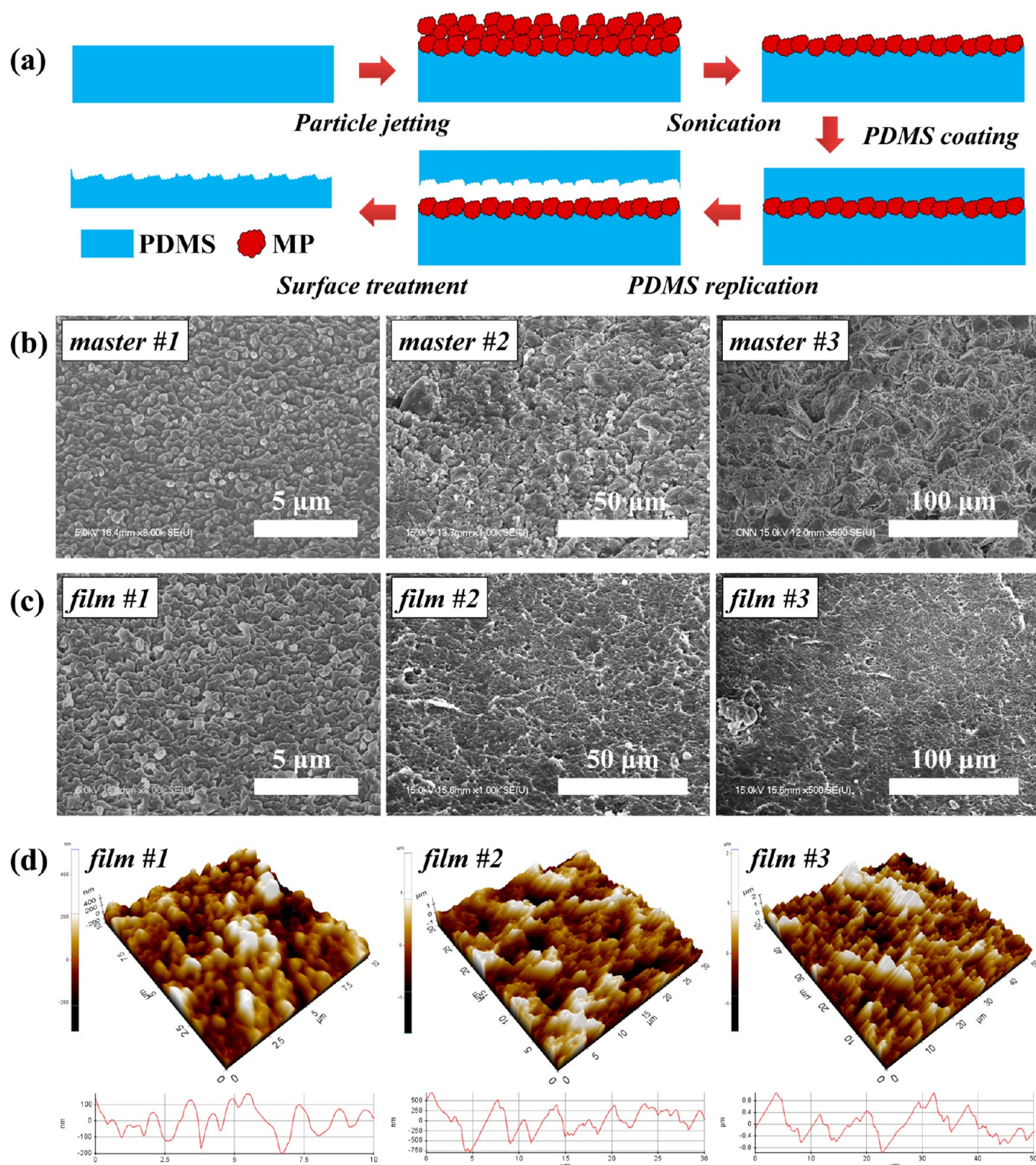


Figure 1. Fabrication of the superhydrophobic PDMS films. (a) Fabrication procedures, (b) particle-embedded masters with differently scaled surface geometries, (c) superhydrophobic PDMS films replicated from the particle-embedded masters of (a), and (d) AFM images of the prepared PDMS films with different surface morphologies.

thanks to several advantages such as simplicity, repeatability and scalability in fabrication, cost-effectiveness (including reusability of masters), and so forth.²⁷ Functional PDMS surface structures with various shapes and length scales ranging from millimeters to sub-micrometers can be easily prepared by negatively replicating the patterns on masters.^{28–37} The development of an efficient method for fabricating the masters

is thus crucial for the achievement of superhydrophobic PDMS surfaces based on the replica molding technique. Thus far, optical lithography techniques capable of obtaining highly accurate and geometrically regular polymeric patterns have been most generally applied to prepare the masters.^{28–33} However, specific process conditions related directly to pattern contrast and expensive equipment are still required for

photosensitive polymers to be patterned on substrates. In addition, it is also quite difficult to avoid fabrication complexity due to the multiple steps of procedures. A laser ablation technique could also be used to readily fabricate masters containing regular patterns even without any lithographic processes by irradiating a laser source directly onto target mold substrates.^{34,35} Nevertheless, this method is still limited by strict and expensive setups, and constraints for large-scale fabrication might arise because laser-based machining processes are generally cumbersome and time-consuming. Besides, substrates with inherent surface roughness such as grit papers and natural lotus leaves were efficiently employed as the masters, contributing greatly to simplifying the overall fabrication procedures.^{36,37} However, surface morphology control of the masters is almost impossible in this approach, which means that the resultant properties of the replicated surfaces also become uncontrollable.

Here, we propose a simple, scalable and cost-effective nonlithographic way of fabricating the masters for demonstrating superhydrophobic PDMS films based on a replica molding technique. The proposed masters were simply prepared by firmly anchoring microparticles (MPs) across the top surface of the PDMS substrate using a facile and scalable abrasive air-jetting (AAJ) technique, followed by curing. In this way, the surface morphology of the PDMS masters can be easily determined depending on the shape and size of the particles, which clearly suggests that the surface morphology of the PDMS films replicated from the PDMS masters can also be easily controlled by using the particles with different shape and size in the AAJ process. Using the proposed PDMS masters, superhydrophobic PDMS films that simultaneously have desirable properties including mechanical flexibility and durability, fairly good optical transparency, controllability of the surface morphology, and low-temperature fabrication were successfully demonstrated.

2. EXPERIMENTAL DETAILS

Fabrication of Superhydrophobic Films. The proposed superhydrophobic PDMS films were simply fabricated by a replica molding technique with microparticle-embedded PDMS masters prepared by a facile and scalable AAJ technique, as illustrated schematically in Figure 1a. A PDMS plate was first prepared and employed as a supporting substrate of the master after accepting MPs. For this, a PDMS prepolymer mixed with a curing agent at a weight ratio of 10:1 was poured onto a silicon substrate after degassing to entirely remove the air bubbles, followed by curing thermally in under-polymerization conditions of PDMS (80 °C for 10 min). The semicuring process is greatly helpful for holding MPs on the PDMS surface by making the surface very sticky. The MPs were then sprayed onto the semicured PDMS surface by the AAJ technique under pressurized conditions at 4 bar. In this study, commercially-available alumina (Al₂O₃) microparticles with different dimensions were employed to control the surface morphology of the PDMS masters. After that, the MPs stuck on the PDMS masters were firmly anchored by completely polymerizing the supporting PDMS substrate at 80 °C for 30 min. The PDMS masters were then sonicated for 30 min to define the surface morphology precisely depending on the shape and size of the MPs used in the process by eliminating the excessive portions attached weakly on the MPs anchored strongly onto the PDMS surface. After that, the replica molding process was conducted to fabricate the superhydrophobic PDMS films with inverted surface morphologies from the MP-embedded PDMS masters. PDMS of 10:1 (base polymer:curing agent) was used after mixing with a volatile solvent (toluene) at a weight ratio of 1:1 to facilitate infiltration and conformity to the layered MPs by lowering the viscosity of the mixture. Subsequently, the PDMS coated on the master was cured

thermally at 80 °C for 30 min, while fully evaporating the solvent components. A thin plasma-polymerized fluorocarbon (PPFC) film based on a continuous C4F8 glow discharge was deposited on the masters as an antiadhesion layer between the solidified PDMS and masters before introducing the mixture onto the PDMS master. Finally, the proposed superhydrophobic PDMS film with 500 μm thickness was prepared by carefully peeling off the solidified PDMS from the master.

Characterization. The surface morphologies of the fabricated particle-embedded PDMS masters and the corresponding superhydrophobic PDMS films were investigated using field emission scanning electron microscopy (FESEM; Hitachi, S4700) and atomic force microscopy (AFM; Park Systems, XE-100).

The wetting properties of the fabricated superhydrophobic PDMS films with different surface morphology were evaluated by characterizing two important criteria: static contact angle (SCA) and contact angle hysteresis (CAH). The measurements of the SCAs and CAHs were performed on more than five different regions of each PDMS film using a contact angle meter (KRÜSS, DSA 20E) equipped with a CCD camera module. Before the measurements, all the prepared PDMS films were coated conformally with the thin-film PPFC to enhance the hydrophobicity by lowering the intrinsic surface energy. The SCAs were measured for deionized (DI) water drops (10 μL in volume) sitting statically on the fabricated films based on a sessile drop technique. To characterize the dynamic wetting behavior of the fabricated PDMS films, the advancing and receding contact angles were first measured while increasing (to 13 μL) and decreasing (to 7 μL) the volume of the water droplet, respectively. The CAHs of the films were obtained from the differences between the measured advancing and receding contact angles.

The optical characteristics of the fabricated PDMS films were investigated in the visible light region with wavelengths ranging from 350 nm to 800 nm using UV visible spectroscopy (SINCO, S310).

Evaluation of Mechanical Robustness. The mechanical robustness of the fabricated superhydrophobic PDMS films was examined under repetitive compressing and stretching conditions using a motorized stage (JISC, JSV-H1000) equipped with a push-pull force gauge (JISC, H-10), while monitoring the wetting properties of the films. The compression test was conducted by applying various levels of force ranging from 1 to 5 N with a 1 N step perpendicularly to the prepared PDMS film using a flat-top metallic tip connected to the force gauge in the motorized system and repetitive compression for up to 500 cycles with a maximum normal force of 5 N. As a further test for the mechanical stability of the PDMS films, their wetting properties were investigated with the application of tensile strain ranging from 10% to 50% with a 10% step at a stretching speed of 100 mm/min. In addition, the films were tested under repetitive stretching for up to 500 cycles with a maximum tensile strain of 50%. For both the cyclic mechanical tests, the SCAs and CAHs of the tested films were measured every 100 cycles.

Self-Cleaning Test. The practical self-cleaning test was conducted by the following procedures. The prepared PDMS film was first attached carefully onto a slide glass (step I). The attached film was then contaminated intentionally by scattering carbon black (CB) nanoparticles with an average diameter of ~50 nm randomly onto its surface (step II). After that, several water droplets were introduced onto the contaminated film by a syringe to make the film clean while tilting it by ~20° (step III). After fully evaporating the residual water components in the PDMS film on a hot plate at 100 °C for 5 min, the optical transmittance of the film at each step was investigated in the visible light wavelengths.

3. RESULTS AND DISCUSSION

Figure 1b shows the SEM images of surfaces of the PDMS masters prepared by the aforementioned fabrication procedures using Al₂O₃ MPs with different average diameters of approximately 1, 10, and 20 μm (denoted as masters #1–#3, respectively, in Figure 1b). The MP layers were stably built on the PDMS supporting substrates with the differently scaled

surface morphologies according to difference in size of the MPs used in the AAI process. The surface morphologies of the prepared masters were transferred successfully onto the PDMS films (denoted as films #1–#3 corresponding to masters #1–#3, respectively) in an inverted manner by the simple replica molding approach, as shown in Figure 1c. The surface morphologies of the prepared PDMS films were further investigated using the AFM. The AFM images in Figure 1d indicate that the PDMS films reveal the differently scaled surface morphologies with the average roughness (R_a) of 66, 247, and 369 nm for films #1, #2, and #3, respectively, depending consistently on those of the masters (see the AFM images of the masters in Figure S1 in the Supporting Information). In addition, the surface morphologies of the PDMS films can also be further controlled by replicating from PDMS masters prepared by the MPs with various shapes and sizes in the proposed approach.

Figure 2a shows the SCAs and CAHs measured on the PDMS films with different morphologies after the PPFC

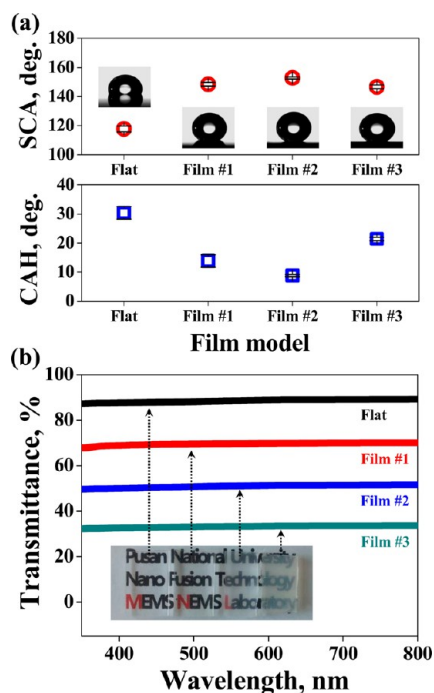


Figure 2. Surface wetting and optical properties measured on the superhydrophobic PDMS films with different surface morphologies. (a) Static contact angle (SCA) and contact angle hysteresis (CAH) (inset: water droplets (10 μ L in volume) placed on each film) and (b) optical transmittance curves (inset: a paper printed with letters underneath each film).

coating. The wetting properties of all the roughened surfaces of the PDMS films were enhanced significantly compared to those of the flat PDMS surface toward both increasing the SCAs and decreasing the CAHs, as shown in Figure 2a. This suggests that the surface roughness on the PDMS films plays a great role in the development of air pockets that can entirely prevent water droplets from touching the bottom surfaces, resulting in reduction of the actual contact area at the interfaces between the surfaces and water droplets, which makes the surfaces superhydrophobic. Under the influence of the surface roughness, the SCA ($148.5 \pm 1.27^\circ$) and CAH ($13.9 \pm 2.11^\circ$) of film #1 (produced from master #1) were enhanced by 26.2 and 54.3

%, respectively, compared to the flat PDMS film. Both the highest SCA ($152.8 \pm 0.67^\circ$) and the lowest CAH ($8.8 \pm 0.43^\circ$) were found on film #2, which indicates that the number of air pockets was more increased, and the actual contact area was more decreased accordingly (with a reduction of solid fraction). This might be because the microscaled valleys in between the MPs on master #2 were transferred onto the PDMS film as protrusions with higher aspect ratio and larger spacing than those of film #1 after replicating. However, the wetting properties of the PDMS films were deteriorated slightly when replicated from the masters decorated with the larger MPs (film #3). In principle, the much larger spacing between the protrusions on film #3 would make it easy for the water droplets to wet the surfaces, resulting in an increase of the solid fraction, which might lead to dominant degradation in the dynamic wetting properties (with ~ 2.4 times higher CAH than film #2).

Figure 2b shows the optical transmittance spectra measured on the PDMS films with different surface morphologies after the PPFC coating. At a wavelength of 550 nm, the optical transmittance of the bare PDMS film was measured to be ~ 88 %. The PDMS film gradually became less transparent as it was roughened, as shown in Figure 2b. This may originate from the fact that the incident light is more scattered at the surface regions as the surface roughness of the film is increased. Nevertheless, letters could be all clearly observed through film #1, which had a transmittance of ~ 70 % at 550 nm wavelength, as shown in the inset in Figure 2b. This suggests that the surface-roughened PDMS films are potentially feasible to be employed as self-cleanable films in glass-based applications owing to their moderate optical transparency and enhanced surface wetting properties.

The reusability of the proposed MP-embedded PDMS masters was tested by repeating the replication process to evaluate the mechanical durability of the masters under repetitive use. Figure 3a shows the SEM images of the PDMS master (master #1) after up to three uses. Significant changes in surface morphology of the master were not observed even after repetitive replications, as shown in Figure 3a and Supporting Information Figure S2 (AFM images). This indicates that the MPs were sufficiently anchored onto the supporting PDMS substrate for them to withstand the replication process without remarkable loss of the MPs, and the release agent (PPFC) coated on the MP layer also played an important role for sufficiently reducing the adhesion force between the anchored MPs and PDMS substrate during release. As a result, the PDMS films (film #1) replicated three times in sequence from the same master showed almost constant performance both in wetting properties and optical transparency, as shown in Figure 3b and c, respectively, due to their similar surface morphologies (see the AFM images of the resultant PDMS films in Supporting Information Figure S3). The experimental observations clearly suggest that the proposed MP-embedded PDMS masters can be used repeatedly without significant degradation in performance of the resultant superhydrophobic PDMS films. This also implies that the proposed approach is practically feasible for making the fabrication of superhydrophobic PDMS films reproducible.

The mechanical robustness of such superhydrophobic surfaces is one of the most crucial requirements for their long-term stability in practical applications. The mechanical stability of the fabricated superhydrophobic PDMS films was examined under repetitive compressing and stretching con-

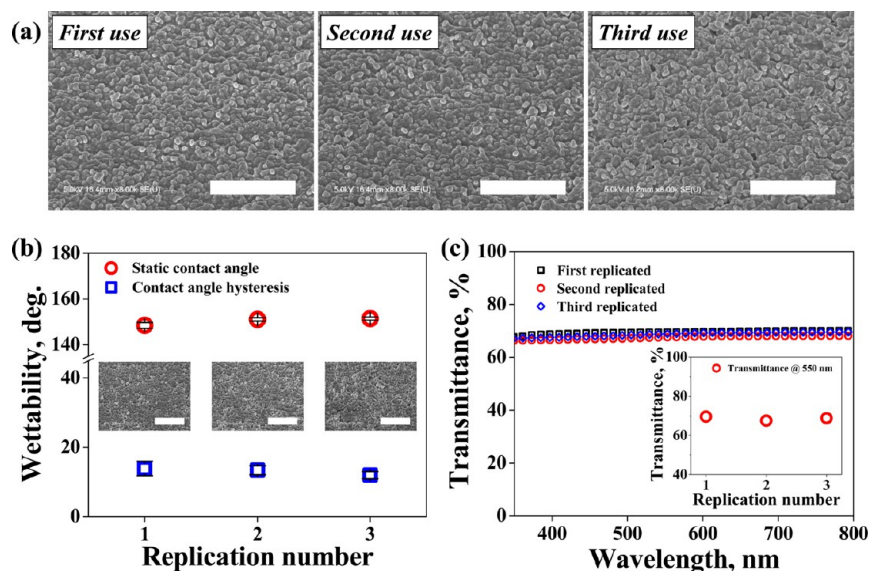


Figure 3. Evaluation of reusability of the particle-embedded masters. (a) SEM images of the master after up to three uses (scale bars: 5 μm), (b) surface wetting properties of the films replicated three times from the same master (inset: SEM images of the resultant PDMS films, scale bars: 5 μm), and (c) optical transmittance characteristics of the prepared PDMS films (inset: transmittance values at a wavelength of 550 nm of each film).

ditions. Figure 4a shows the average SCAs of the PDMS film (film #1), which were normalized with respect to the initial contact angle, due to the applied normal force ranging from 1 to 5 N with a 1 N step and repetitive compression for up to 500 cycles with a maximum normal force of 5 N (inset graph in Figure 4a). The static wetting property of the PDMS film was

retained almost constantly with negligible deviations less than 0.4 % even under the repetitive compressing deformations, as shown in Figure 4a.

Figure 4b shows the normalized average SCAs of the PDMS film (film #1) as a function of tensile strain ranging from 10% to 50% with a 10% step. The inset graph in Figure 4b shows the normalized SCAs measured every 100 cycles during stretching for up to 500 cycles with a maximum tensile strain of 50% at a loading speed of 100 mm/min. The static wetting property of the PDMS film was also found to be stable after the mechanical stretching tests. Under both the compression and stretching tests, the dynamic wetting property (CAH) of the PDMS film was also maintained without appreciable discrepancies, as shown in Supporting Information Figure S4. Moreover, no significant changes in the surface morphologies of the films were observed after the mechanical tests, as shown in Supporting Information Figure S5. The mechanical robustness of the superhydrophobic PDMS films can mostly be attributed to the fact that all the parts (surface structures and supporting substrates) of the superhydrophobic films are composed homogeneously of highly elastic PDMS, resulting in reliable performance.

Figure 5a shows the PDMS films attached on various glass-based products with curved surfaces. The PDMS films were easily laminated onto the glass products without tapes or adhesives, ensuring good coverage due to their thin and compliant architectures. To demonstrate the practical usability of the superhydrophobic PDMS films, a self-cleaning test was carried out after attaching them to a slide glass. Figure 5b shows the optical transmittance curves of the superhydrophobic PDMS film at each step (denoted as step I (as-prepared), step II (contaminated), and step III (cleaned)) with digital images of the film under each surface state. The optical transmittance measured at a wavelength of 550 nm for the superhydrophobic PDMS film at each step is summarized in Figure 5c. The transmittance of the PDMS film was severely degraded ($\sim 90\%$ degradation) after being contaminated by losing a number of paths of incident light (see the middle image in the inset in Figure 5b). After the simple cleaning process, the transmittance

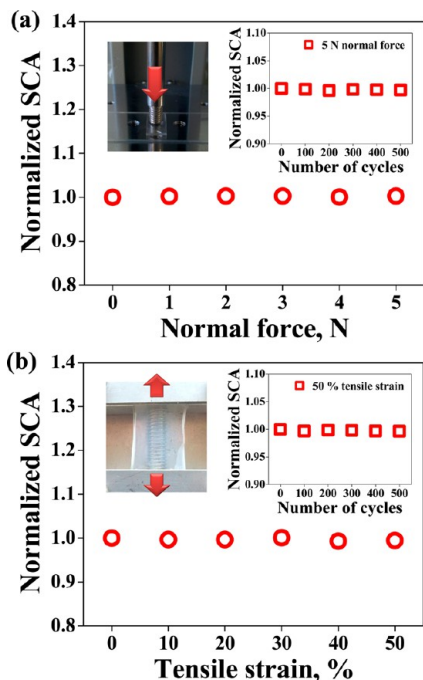


Figure 4. Normalized average SCAs of the superhydrophobic PDMS film (film #1). (a) Due to normal force application under various loading forces ranging from 1 to 5 N with a 1 N step (inset graph: due to repetitive compressing up to 500 cycles with a maximum force of 5 N) and (b) due to stretching under various tensile strains ranging from 10% to 50% with a 10 % step (inset graph: due to repetitive stretching up to 500 cycles with a maximum tensile strain of 50% at a loading speed of 100 mm/min.).

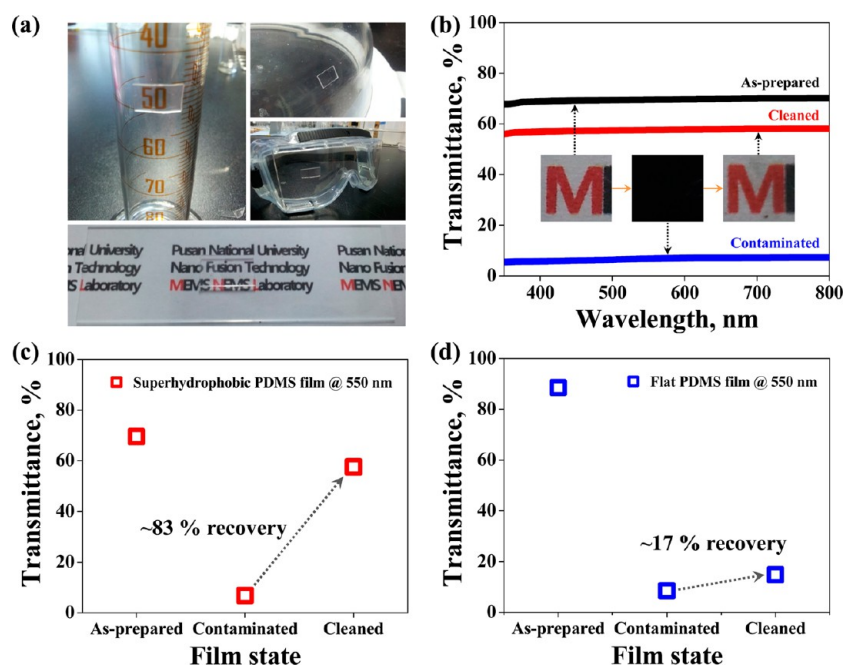


Figure 5. Practical demonstration of the superhydrophobic PDMS film (film #1). (a) Digital images of the PDMS films attached to various glass products, (b) optical transmittance characteristics of the PDMS film attached on slide glasses under as-prepared, contaminated, and cleaned conditions (inset: digital images of the PDMS film under each condition), and (c, d) transmittance values at a wavelength of 550 nm of the superhydrophobic and flat PDMS films, respectively, under as-prepared, contaminated, and cleaned conditions.

was recovered $\sim 83\%$ with respect to that of the as-prepared PDMS film due to its water-repellent surface property (see the rightmost image in the inset in Figure 5b). For comparison, the self-cleaning test was conducted for a flat PDMS film under the same procedures described above. After cleaning, the corresponding optical transmittance at a wavelength of 550 nm of the flat PDMS film was recovered only $\sim 17\%$ compared to that in the as-prepared state, as shown in Figure 5d. These results clearly demonstrate the potential of the proposed superhydrophobic PDMS films to be employed practically in glass-based applications based on their easy attachability to glass and self-cleaning capability.

4. CONCLUSION

In summary, we have presented a simple method to demonstrate a class of superhydrophobic PDMS surfaces that are potentially applicable to glass-based systems even with complex surfaces. The AAJ technique makes it possible to fabricate the PDMS masters in a simple and cost-effective manner by simply embedding the MPs onto the surfaces of PDMS substrates. The surface morphologies of the PDMS masters could be tailored simply by using MPs with different shape or size in the AAJ process. In this way, we have successfully realized superhydrophobic PDMS films with different levels of surface morphologies through a standard soft-lithographic replication process. The fabricated PDMS films showed good surface wetting properties (SCA of $148.5 \pm 1.27^\circ$, CAH of $13.9 \pm 2.11^\circ$ for film #1) and fair optical transparency ($\sim 70\%$ at a wavelength of 550 nm for film #1), and were robust against both repetitive compression (under a normal force of 5 N for 500 cycles) and stretching (under tensile strain of 50% 500 cycles) with almost no degradation in performance owing to their all-elastomeric architectures. Furthermore, the PDMS films replicated multiple times from the same master revealed no significant disparities in both

wetting and optical properties thanks to the mechanical durability of the PDMS masters. As a potential application, the self-cleaning capability of the fabricated superhydrophobic PDMS films was successfully demonstrated by attaching it onto a slide glass. The optical transmittance of the contaminated PDMS film was recovered $\sim 83\%$ with respect to that in the initial state after cleaning. We believe that the unique non-lithographic method is highly feasible for use as an efficient route for the preparation of superhydrophobic PDMS films in diverse practical applications due to the simplicity and rapidness of fabrication, as well as the cost-effectiveness, potential scalability, and reproducibility in the process.

■ ASSOCIATED CONTENT

Supporting Information

AFM images of the particle-embedded masters with differently scaled surface geometries (masters #1–#3) (Figure S1); AFM images of the masters (master #1) after up to three uses (Figure S2); AFM images of the superhydrophobic PDMS film (film #1) replicated three times from the same master (Figure S3); CAHs of the PDMS film due to compressing and stretching deformations (Figure S4); SEM images of the PDMS film (film #1) before and after repetitive compressing (500 cycles) and stretching (500 cycles) tests (Figure S5). This material is available free of charge via the Internet at <http://pubs.acs.org>.

■ AUTHOR INFORMATION

Corresponding Author

*E-mail: jongkim@pusan.ac.kr.

Author Contributions

^{||}D.-W.J. and S.-J.K. contributed equally.

Notes

The authors declare no competing financial interest.

ACKNOWLEDGMENTS

This work was supported by “Development of Next Generation Multi-functional Machining Systems for Eco/Bio Components” project of Ministry of Knowledge Economy.

REFERENCES

- (1) Yao, X.; Song, Y.; Jiang, L. Applications of Bio-Inspired Special Wettable Surfaces. *Adv. Mater.* **2011**, *23*, 719–734.
- (2) Xue, C.-H.; Jia, S.-T.; Zhang, J.; Ma, J.-Z. Large-area fabrication of superhydrophobic surfaces for practical applications: an overview. *Sci. Technol. Adv. Mater.* **2010**, *11*, 033002.
- (3) Crick, C. R.; Parkin, I. P. Preparation and Characterisation of Super-Hydrophobic Surfaces. *Chem.—Eur. J.* **2010**, *16*, 3568–3588.
- (4) Zhang, X.; Shi, F.; Niu, J.; Jiang, Y.; Wang, Z. Superhydrophobic surfaces: from structural control to functional application. *J. Mater. Chem.* **2008**, *18*, 621–633.
- (5) Li, X.-M.; Reinhoudt, D.; Crego-Calama, M. What do we need for a superhydrophobic surface? A review on the recent progress in the preparation of superhydrophobic surfaces. *Chem. Soc. Rev.* **2007**, *36*, 1350–1368.
- (6) Guo, Z.; Liu, W.; Su, B.-L. Superhydrophobic surfaces: From natural to biomimetic to functional. *J. Colloid Interface Sci.* **2011**, *353*, 335–355.
- (7) Zhang, Y.-L.; Xia, H.; Kim, E.; Sun, H.-B. Recent developments in superhydrophobic surfaces with unique structural and functional properties. *Soft Matter* **2012**, *8*, 11217–11231.
- (8) Bhushan, B.; Jung, Y. C. Natural and biomimetic artificial surfaces for superhydrophobicity, self-cleaning, low adhesion, and drag reduction. *Prog. Mater. Sci.* **2011**, *56*, 1–108.
- (9) Wisdom, K. M.; Watson, J. A.; Qu, X.; Liu, F.; Watson, G. S.; Chen, C.-H. Self-cleaning of superhydrophobic surfaces by self-propelled jumping condensate. *Proc. Natl. Acad. Sci. U.S.A.* **2013**, *110*, 7992–7997.
- (10) Truesdell, R.; Mammoli, A.; Vorobief, P.; Swol, F. v.; Brinker, C. J. Drag Reduction on a Patterned Superhydrophobic Surface. *Phys. Rev. Lett.* **2006**, *97*, 044504.
- (11) Farhadi, S.; Farzaneh, M.; Kulinich, S. A. Anti-icing performance of superhydrophobic surfaces. *Appl. Surf. Sci.* **2011**, *257*, 6264–6269.
- (12) Ivanova, E. P.; Hasan, J.; Webb, H. K.; Truong, V. K.; Watson, G. S.; Watson, J. A.; Baulin, V. A.; Pogodin, S.; Wang, J. Y.; Tobin, M. J.; Løbbe, C.; Crawford, R. J. Natural Bactericidal Surfaces: Mechanical Rupture of *Pseudomonas aeruginosa* Cells by Cicada Wings. *Small* **2012**, *8*, 2489–2494.
- (13) Roach, P.; Shirtcliffe, N. J.; Newton, M. I. Progress in superhydrophobic surface development. *Soft Matter* **2008**, *4*, 224–240.
- (14) Yan, Y. Y.; Gao, N.; Barthlott, W. Mimicking natural superhydrophobic surfaces and grasping the wetting process: A review on recent progress in preparing superhydrophobic surfaces. *Adv. Colloid Interface Sci.* **2011**, *169*, 80–105.
- (15) Celia, E.; Darmanin, T.; Taffin de Givenchy, E.; Amigoni, S.; Guittard, F. Recent advances in designing superhydrophobic surfaces. *J. Colloid Interface Sci.* **2013**, *402*, 1–18.
- (16) Darmanin, T.; Taffin de Givenchy, E.; Amigoni, S.; Guittard, F. Superhydrophobic Surfaces by Electrochemical Processes. *Adv. Mater.* **2013**, *25*, 1378–1394.
- (17) Wang, X.; Ding, B.; Yu, J.; Wang, M. Engineering biomimetic superhydrophobic surfaces of electrospun nanomaterials. *Nano Today* **2011**, *6*, 510–530.
- (18) Tropmann, A.; Tanguy, L.; Koltay, P.; Zengerle, R.; Riegger, L. Completely Superhydrophobic PDMS Surfaces for Microfluidics. *Langmuir* **2012**, *28*, 8292–8295.
- (19) Hwang, S. J.; Oh, D. J.; Jung, P. G.; Lee, S. M.; Go, J. S.; Kim, J.-H.; Hwang, K.-Y.; Ko, J. S. Dry etching of polydimethylsiloxane using microwave plasma. *J. Micromech. Microeng.* **2009**, *19*, 095010.
- (20) Manca, M.; Cortese, B.; Viola, I.; Aricò, A. S.; Cingolani, R.; Gigli, G. Influence of Chemistry and Topology Effects on Superhydrophobic CF₄-Plasma-Treated Poly(dimethylsiloxane) (PDMS). *Langmuir* **2008**, *24*, 1833–1843.
- (21) Tserepi, A. D.; Vlachopoulou, M. -E.; Gogolides, E. Nano-texturing of poly(dimethylsiloxane) in plasmas for creating robust super-hydrophobic surfaces. *Nanotechnology* **2006**, *17*, 3977–3983.
- (22) Yong, J.; Chen, F.; Yang, Q.; Zhang, D.; Bian, H.; Du, G.; Si, J.; Meng, X.; Hou, X. Controllable Adhesive Superhydrophobic Surfaces Based on PDMS Microwell Arrays. *Langmuir* **2013**, *29*, 3274–3279.
- (23) Jin, M.; Feng, X.; Xi, J.; Zhai, J.; Cho, K.; Feng, L.; Jiang, L. Super-Hydrophobic PDMS Surface with Ultra-Low Adhesive Force. *Micromol. Rapid Commun.* **2005**, *26*, 1805–1809.
- (24) Khorasani, M. T.; Mirzadeh, H.; Kermani, Z. Wettability of porous polydimethylsiloxane surface: morphology study. *Appl. Surf. Sci.* **2005**, *242*, 339–345.
- (25) Taffin de Givenchy, E. P.; Amigoni, S.; Martin, C.; Andrada, G.; Caillier, L.; Gèribaldi, S.; Guittard, F. Fabrication of Superhydrophobic PDMS Surfaces by Combining Acidic Treatment and Perfluorinated Monolayers. *Langmuir* **2009**, *25*, 6448–6453.
- (26) Wu, J.; Bai, H.-J.; Zhang, X.-B.; Xu, J.-J.; Chen, H.-Y. Thermal/Plasma-Driven Reversible Wettability Switching of a Bare Gold Film on a Poly(dimethylsiloxane) Surface by Electroless Plating. *Langmuir* **2010**, *26*, 1191–1198.
- (27) Xia, Y.; Whitesides, G. M. Soft Lithography. *Angew. Chem., Int. Ed.* **1998**, *37*, 550–575.
- (28) Im, M.; Im, H.; Lee, J.-H.; Yoon, J.-B.; Choi, Y.-K. A robust superhydrophobic and superoleophobic surface with inverse-trapezoidal microstructures on a large transparent flexible substrate. *Soft Matter* **2010**, *6*, 1401–1404.
- (29) Kim, D. S.; Lee, B.-K.; Yeo, J.; Choi, M. J.; Yang, W.; Kwon, T. H. Fabrication of PDMS micro/nano hybrid surface for increasing hydrophobicity. *Microelectron. Eng.* **2009**, *86*, 1375–1378.
- (30) Guo, S. S.; Sun, M. H.; Shi, J.; Liu, Y. J.; Huang, W. H.; Combellas, C.; Chen, Y. Patterning of hydrophilic micro arrays with superhydrophobic surrounding zones. *Microelectron. Eng.* **2007**, *84*, 1673–1676.
- (31) Park, Y.-B.; Im, H.; Im, M.; Choi, Y.-K. Self-cleaning effect of highly water-repellent microshell structures for solar cell applications. *J. Mater. Chem.* **2011**, *21*, 633–636.
- (32) Cortese, B.; D’Amone, S.; Manca, M.; Viola, I.; Cingolani, R.; Gigli, G. Superhydrophobicity Due to the Hierarchical Scale Roughness of PDMS Surfaces. *Langmuir* **2008**, *24*, 2712–2718.
- (33) Liu, X.; Luo, C. Fabrication of super-hydrophobic channels. *J. Micromech. Microeng.* **2010**, *20*, 025029.
- (34) Holgerson, P.; Sutherland, D. S.; Kasemo, B.; Chakarov, D. Patterning and modification of PDMS surface through laser micro-machining of silicon masters and molding. *Appl. Phys. A* **2005**, *81*, 51–56.
- (35) Yoon, T. O.; Shin, H. J.; Jeoung, S. C.; Park, Y.-I. Formation of superhydrophobic poly(dimethylsiloxane) by ultrafast laser-induced surface modification. *Opt. Express* **2008**, *16*, 12715.
- (36) Stanton, M. M.; Bucker, R. E.; MacDonald, J. C.; Lambert, C. R.; McGimpsey, W. G. Super-hydrophobic, highly adhesive, polydimethylsiloxane (PDMS) surfaces. *J. Colloid Interface Sci.* **2012**, *367*, 502–508.
- (37) Liu, C. Rapid fabrication of microfluidic chip with three-dimensional structures using natural lotus leaf template. *Microfluid. Nanofluid.* **2010**, *9*, 923–931.